LA-UR-22-20261

Approved for public release; distribution is unlimited.

Title:	238PuO2 In Vitro Lung Dissolution Rate and Particle Size Determination for Material Involved in the June 8, 2020 Incident at the Los Alamos National Laboratory PF-4 Facility
Author(s):	Lamont, Stephen Philip; Steiner, Robert Ernest; Macsik, Zsuzsanna; Hudston, Lisa Ann; Harris, Michael Nathan; Tenner, Travis Jay; Naes, Benjamin Elliott; Wurth, Kimberly Nicole
Intended for:	Report
Issued:	2022-01-12

^{238}PuO$_2$ *In Vitro* Lung Dissolution Rate and Particle Size Determination for Material Involved in the June 8, 2020 Incident at the Los Alamos National Laboratory PF-4 Facility

Final Report

May 20, 2021

Contributors:

Zsuzsanna Macsik, Lisa Hudston & Mike Harris

Radiochemistry, Alpha Spectrometry, and Radiography

Travis Tenner, Benjamin Naes, & Kimberly Wurth

Electron Microscopy and Particle Characterization

Stephen LaMont & Robert Steiner

Technical Direction and Management

Nuclear and Radiochemistry

Executive Summary

As part of the LANL response to the June 8, 2020 ^{238}PuO$_2$ inhalation exposure incident in PF-4, the Nuclear and Radiochemistry Group (C-NR) was asked to assist in determining the lung dissolution rate and particle size distribution of the airborne material. These material characteristics, along with urine and fecal bioassay data, are used by the Radiation Protection Services (RP-SVS) internal dosimetrists to refine dose estimates for exposed workers. Similar to previous studies, an *in vitro* lung dissolution rate study was performed to assess how fast ^{238}Pu is cleared from the lungs. Given that PuO$_2$ is a relatively insoluble material, it dissolves very slowly and requires *in vitro* studies of 100 or more days to estimate dissolution rates. This report details the results of a 100 day *in vitro* dissolution rate study and the particle size characteristics of ^{238}PuO$_2$ collected on an air filters during the incident.

Results show that the ^{238}PuO$_2$ involved in this incident has behavior comparable to PuO$_2$ from previous *in vitro* studies, with approximately 1% of material dissolving quickly, and 99% of the material dissolving very slowly, with a half-time of approximately 120 years. This is somewhat slower than what was determined in a previous study of LANL ^{238}PuO$_2$ [1], which had an experimental dissolution half-time of 3 years, but significantly faster than 3000 years measured for ^{239}PuO$_2$ [2]. Particle size distribution measurements indicate that particle sizes range from 0.10 μm – 6 μm, with most < 2 μm, which is reasonable based on our understanding of the process history of the ^{238}PuO$_2$. Particle size, specific surface area, calcining temperature, specific activity, and age all are known factors that can impact the dissolution rate of refractory materials, however, there are too few studies to quantify the exact influence of these parameters on a measured dissolution rate. The results of this study add to that knowledge base, and provide new insights into the dissolution rates for this LANL process-specific ^{238}PuO$_2$ material.

1. Background

An incident occurred on June 8, 2020 at the Los Alamos National Laboratory PF-4 facility that resulted in confirmed and potential inhalation exposures to $^{238}PuO_2$ in fine powder form. To assist dose estimates, RP-Division requested C-Division assistance to determine the *in vitro* lung dissolution rate and particle size distribution of the $^{238}PuO_2$ in samples collected at the time of the incident. This report presents the preliminary findings for the first 20 days of the *in vitro* study, along with particle size analysis work completed to date. A second report with updated results will be provided upon completion of the study.

2. Samples

A total of 12 samples were provided to C-NR for this work, including:
- Seven fixed head air sampler (FAS) filters,
- Three continuous air monitoring (CAM) filters,
- Two pieces of the personal protective equipment (PPE) worn during the incident by the employee with the highest exposure.

3. Initial screening with autoradiography

Digital autoradiography was used to determine the distribution of radioactivity in the air filter and PPE samples. Samples were exposed approximately 24 hours to digital film sensitive to alpha particles, and read using a GE Typhoon radiography system. Images were assigned a false color gradient that scales from blue background to red in areas with the high alpha intensity. Results confirmed that $^{238}PuO_2$ particles were relatively evenly dispersed over the air filters (Figure 1), although there was a large variation in the activity of ^{238}Pu between filters. Particle rich areas of contamination were present on the samples cut from the PPE worn by the individual with the inhalation intake (Figure 2).
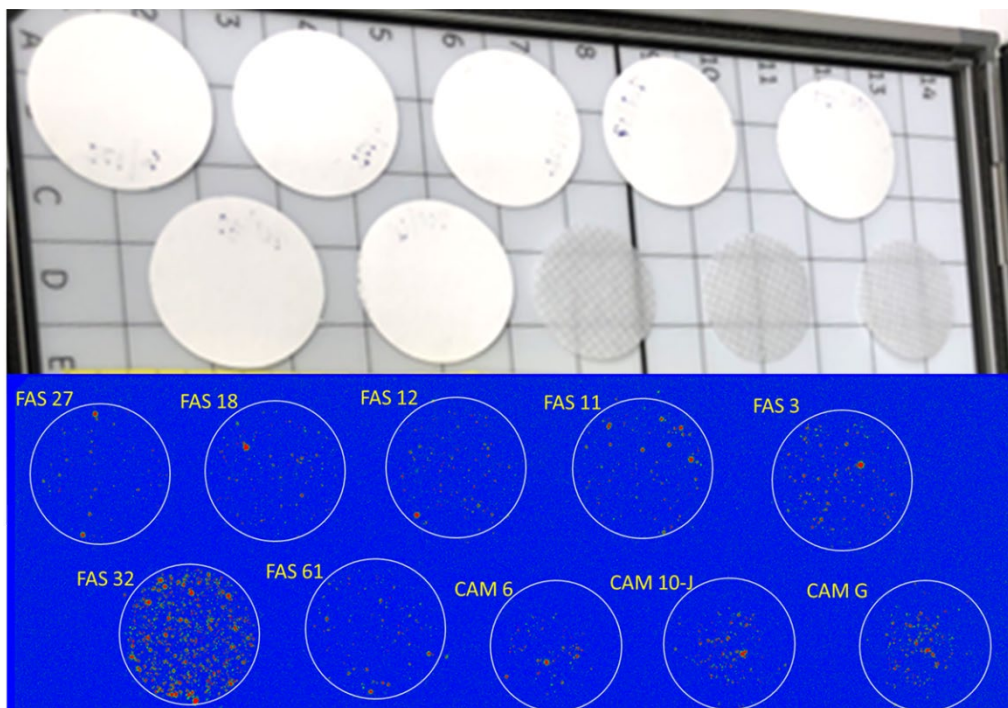

Figure 1: Photograph and radiograph of FAS and CAM filters showing the spatial distribution of alpha activity.
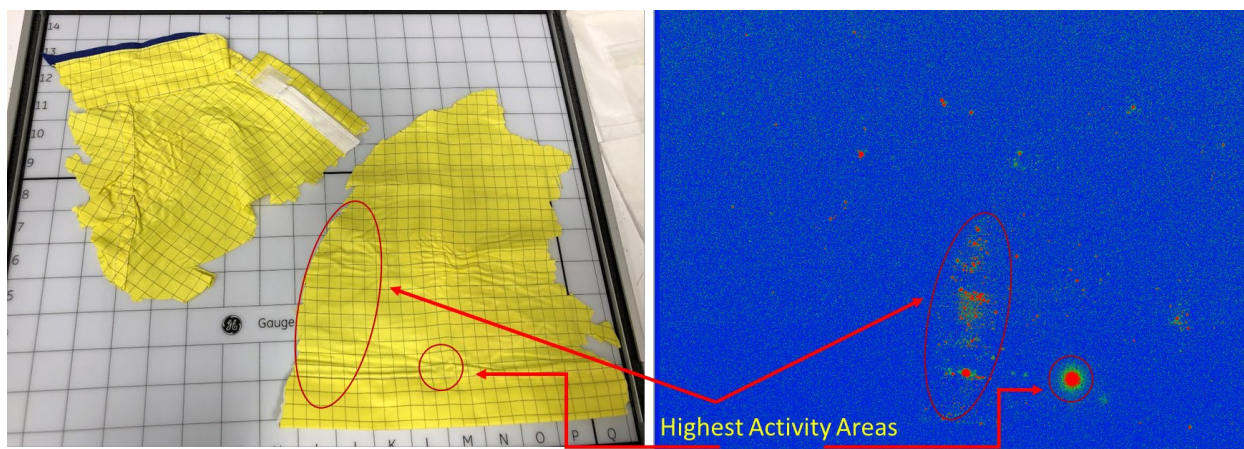

Figure 2: Photograph and radiograph of PPE samples showing the spatial distribution of alpha activity.

4. Particle size analysis with alpha spectrometry, autoradiography and scanning electron microscopy (SEM)

Sample preparation of ashed PPE mounts

One of the PPE samples was especially rich in particles, and was selected for the particle size analysis completed to date. All sample preparation work was performed in a glove bag within a fume hood for initial sample processing, or a fume hood for later steps where dispersal of Pu was less likely. Using the radiograph as a guide, two sub-samples of PPE were cut from the larger sample and placed into quartz tubes. The quartz tubes containing the PPE were capped and moved to a muffle furnace, where they were heated to 525 °C for 24 hours, a temperature low enough that it should have minimal impact on particle morphology. This rendered the PPE into a fine, light-gray ash. Upon cooling and removal from the furnace, a transfer pipette was used to add approximately 5 mL methanol to each quartz tube containing ash. The methanol + ashed PPE suspension from each quartz tube was then removed using the transfer pipette, and was transferred into a 22 mL Savillex container. This served as the stock solution of particles for further subsampling.

Alpha spectrometry, autoradiography, and scanning electron microscopy require flat, wafer-like surfaces for analysis. To achieve this, mounts were prepared by adhering a ½" diameter circular piece of carbon tape to the center of a 1" diameter stainless steel disk (~1 mm thickness). Using a hotplate set to 75 °C, small aliquots (50-100 µL increments) of the methanol + ashed PPE suspension were iteratively pipetted onto the carbon tape; the elevated temperature of the hotplate surface allowed for gentle but rapid drying of the methanol, leaving behind a thin ash layer adhered to the carbon tape. The methanol + PPE suspension were placed in an ultrasonic bath for 5 minutes prior to pipetting to assist in removing representative subsamples of particles. The mount was iteratively counted by alpha spectrometry, with a goal of achieving a total activity near, but not exceeding, 2500 dpm; this activity limit was chosen to minimize any potential for contamination, although the PPE ash was well-adhered to the mount.

Scanning Electron Microscopy

Six ashed PPE mounts were investigated for the presence of [238]Pu-containing particles by SEM. All mounts were carbon coated to minimize charging of the SEM electron beam, and to further bind the ashed PPE to the mount. Pieces of copper tape were used to connect the mount surfaces to the sample stage, to further minimize charging. Backscattered electron (BSE) imaging was used to locate particles, with a resolution of ~0.050 µm (e.g. Figure 3), as higher atomic number species (higher Z) appear brighter than lower atomic number (lower Z) species. Thus, optimal imaging of only the highest Z phases was accomplished by adjusting the brightness and contrast of BSE imaging. An example of a BSE image optimized to locate Pu particles within the ash is shown in Figure 4.

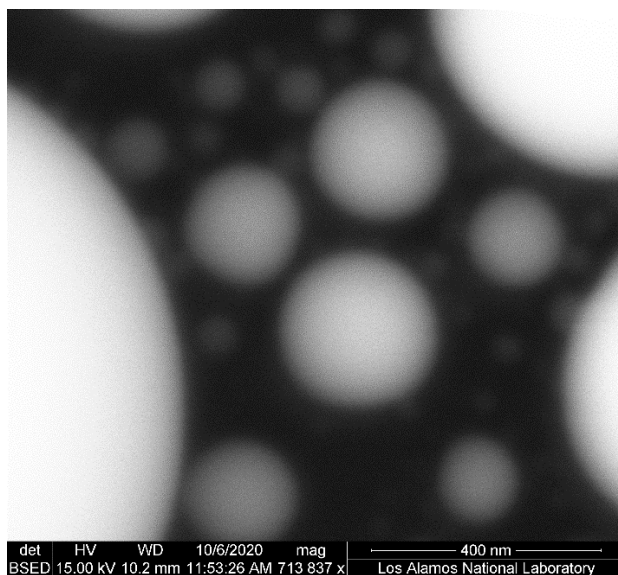**Figure 3: BSE image of tin spheres from a calibration sample, illustrating a particle size resolution of ~0.050 μm.**
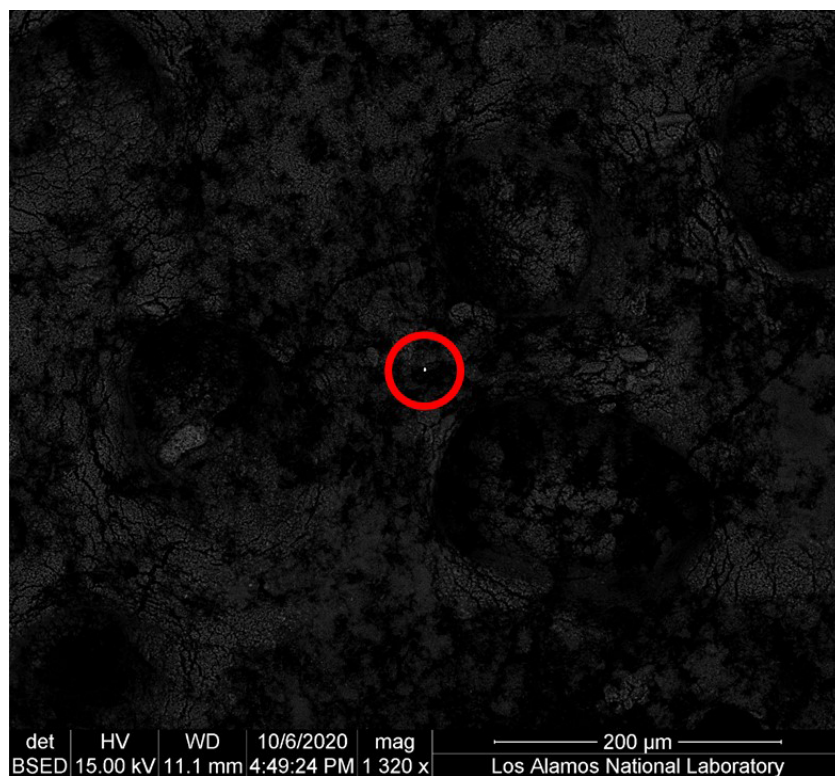

Figure 4: Example SEM BSE image, illustrating brightness and contrast settings that allow for a high Z Pu particle to appear very bright (center of red circle in the figure) among a matrix of darker appearing, lower Z materials within the ashed PPE.

Corresponding autoradiographs of each mount proved highly useful as a tool to navigate to higher-activity regions, where Pu-bearing particles could be located and imaged with the SEM. An example of navigational workflow is shown in Figure 5. Starting with an autoradiograph (Figure 5a), regions showing the highest activity (largest blue signal regions in Figure 5a) were selected as regions to investigate by SEM imaging (e.g. Figure 5b). A relatively low magnification setting was used to scan over the targeted area, in order to locate particles with a high Z signature (e.g. Figure 5b). Once a particle of interest was identified, a higher magnification was employed for imaging (e.g. Figure 5c), and energy dispersive spectroscopy (EDS) was used to determine if the particle did or did not consist of Pu. Figure 5d shows an example of an EDS spectrum containing prominent peaks corresponding to Pu, where lesser peaks from other species are those from other PPE ash matrix material within the EDS interaction volume (approximately a 2 μm diameter sphere). We note that many autoradiograph activity areas likely did not correspond to Pu, as evidenced by other activity-generating particles (e.g. U) identified within the PPE ashed material. For example, even though each mount was thoroughly scanned over its entirety, we found only one to three Pu-bearing particles per mount. In addition, Pu-bearing particles were mainly found in areas of an autoradiograph showing the most activity.
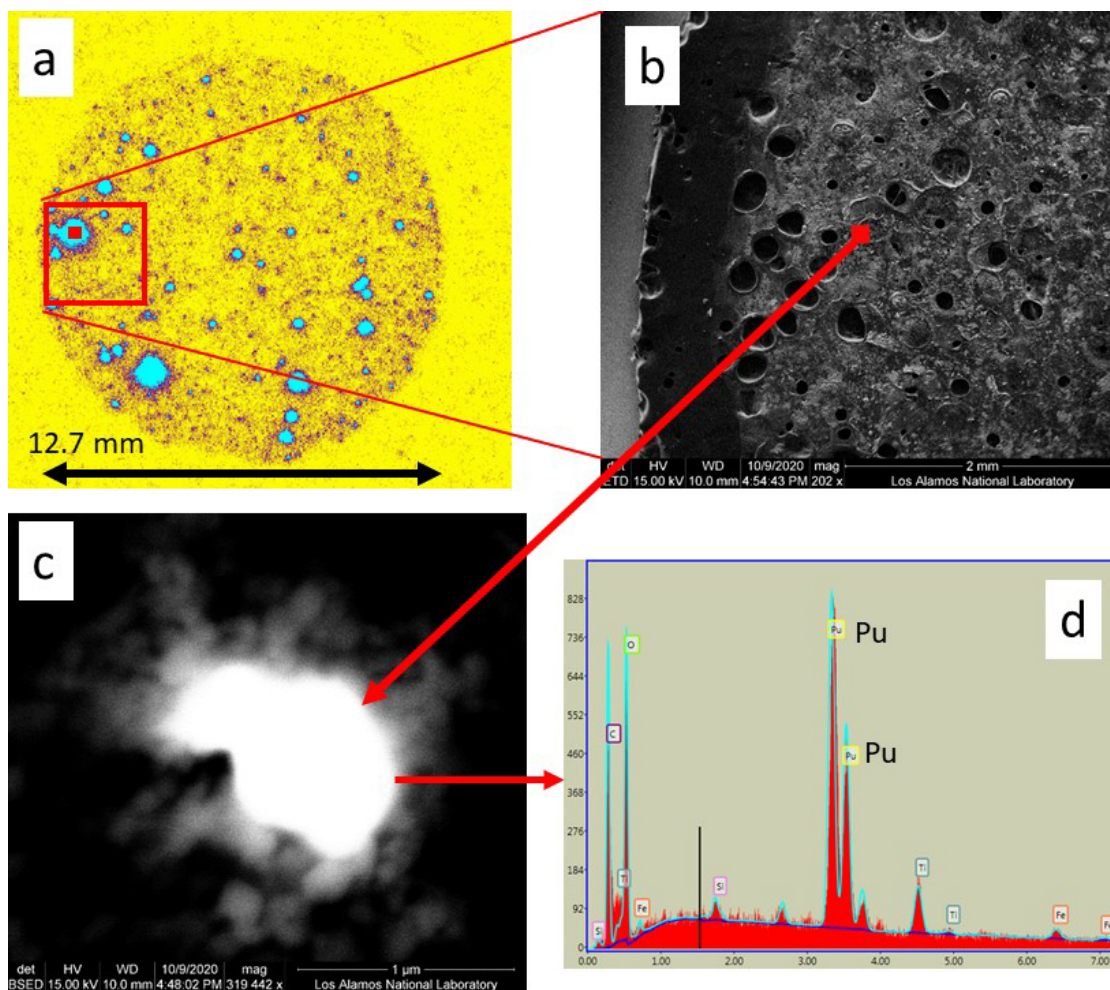

Figure 5: Example workflow for locating Pu-bearing particles. Starting with autoradiography (a), regions of high activity are targeted (b). Once high Z particles are located (bright BSE, panel c), EDS is performed to determine whether or not the particle contains Pu (d).

SEM results

A total of 11 Pu-bearing particles were identified from the six mounts. Autoradiographs of each mount, and the corresponding activity areas from where Pu-bearing particles were found, are shown in Figure 6. SEM BSE images of the particles are shown in Figure 7, and are labeled according to their autoradiograph signatures per sample. Particles ranged from 0.38 μm to 6.2 μm in size, with dimensions given in Table 1.
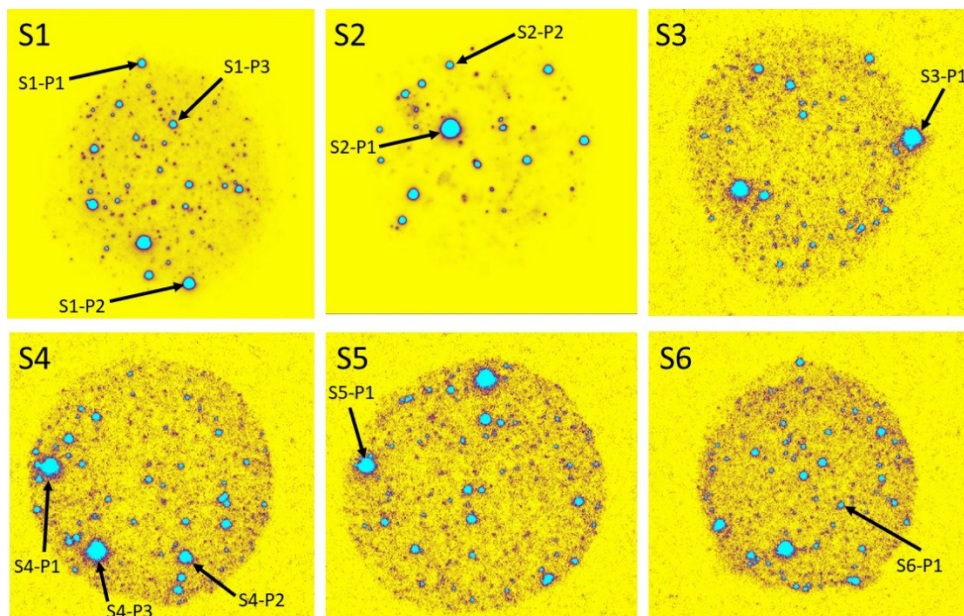
Figure 6: Autoradiographs of the six mounts investigated by SEM. Arrowed locations correspond to areas were Pu-bearing particles were found, and the labeling corresponds to those in the SEM images in Figure 7.

Table 1: Pu particle sizes from SEM imaging

Sample ID	Particle ID	Dimension 1	Dimension 2
S1	P1	0.98 μm	0.56 μm
	P2	2.67 μm	1.60 μm
	P3	1.20 μm	0.56 μm
S2	P1	6.16 μm	1.90 μm
	P2	0.96 μm	0.73 μm
S3	P1	2.02 μm	1.15 μm
S4	P1	1.07 μm	0.76 μm
	P2	0.77 μm	0.38 μm
	P3	0.78 μm	0.48 μm
S5	P1	2.08 μm	1.68 μm
S6	P1	0.79 μm	0.59 μm

Figure 7: SEM BSE images of located Pu-bearing particles. Labeling of particles is consistent with the autoradiographs in Figure 6.

Combined radiography and SEM particle size analysis

The radiography images of samples S1 and S2 were further analyzed to establish a correlation between the damage volume in the radiography film for each significant particle present and the size of each particle. In this process, each particle of significant activity is identified in the radiograph and numbered (Figure 8), and the damage volume in the film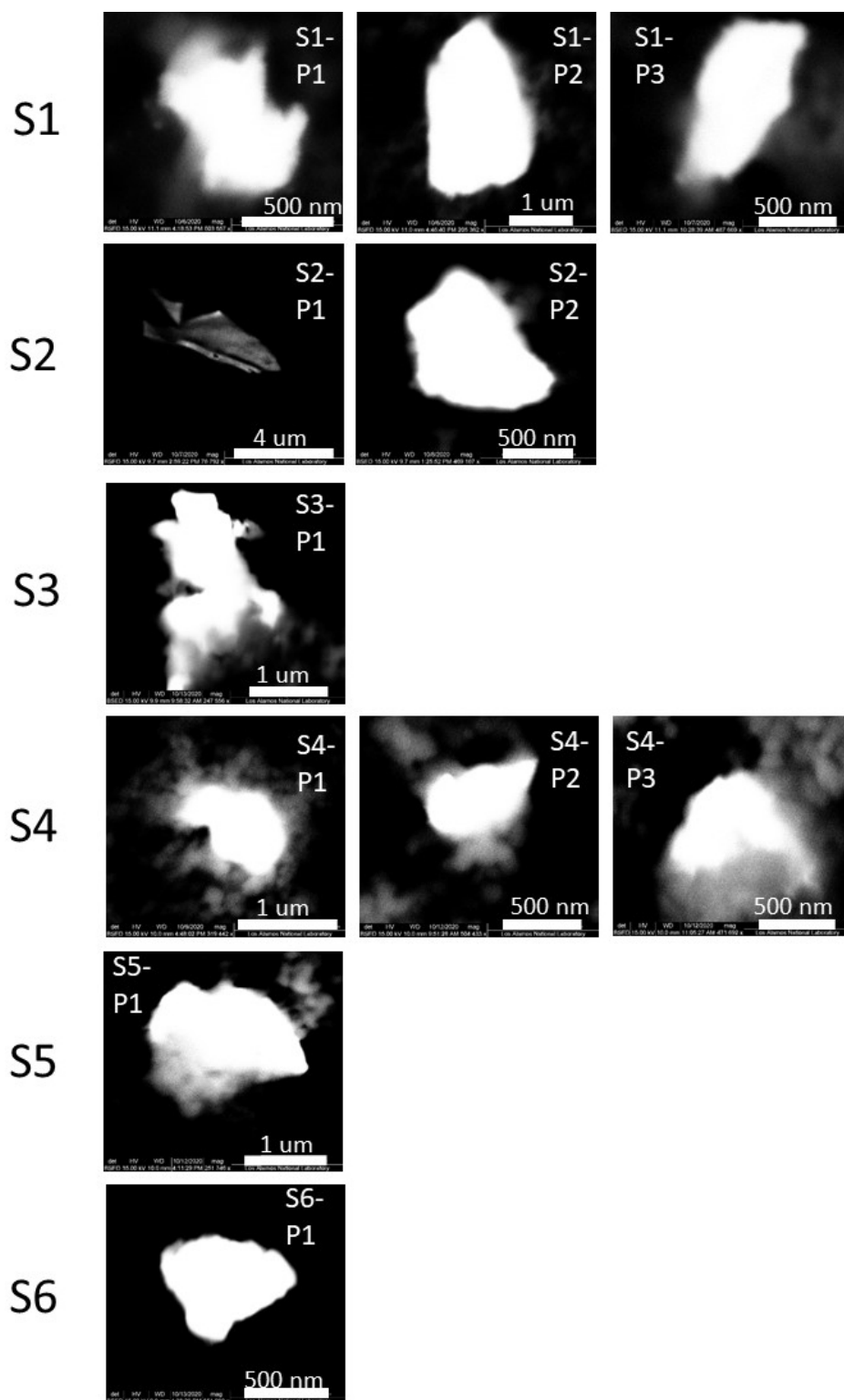 is calculated using GE's proprietary image analysis software. The damage volume of each particle is normalized, and the distribution is used to calculate the ^{238}Pu present in each particle as a fraction of the total ^{238}Pu activity measured by alpha spectrometry. The individual particle activity is converted back to a particle size using the theoretical density of ^{238}PuO$_2$ (11.3 g/cm^3). There are some important assumptions in this approach, including that particles are spherical, all activity present is in the form of discrete particles of PuO$_2$, and that all particles contributing significantly to the radiography signal are included in the analysis. Regarding the first assumption, it is possible that agglomerates of particles are present, however, these agglomerates should behave as single particles from a inhalation dosimetry perspective, where the AMAD of the agglomerate determines where the particle deposits in the respiratory tract. Particles of pure uranium were found by SEM, but the activity
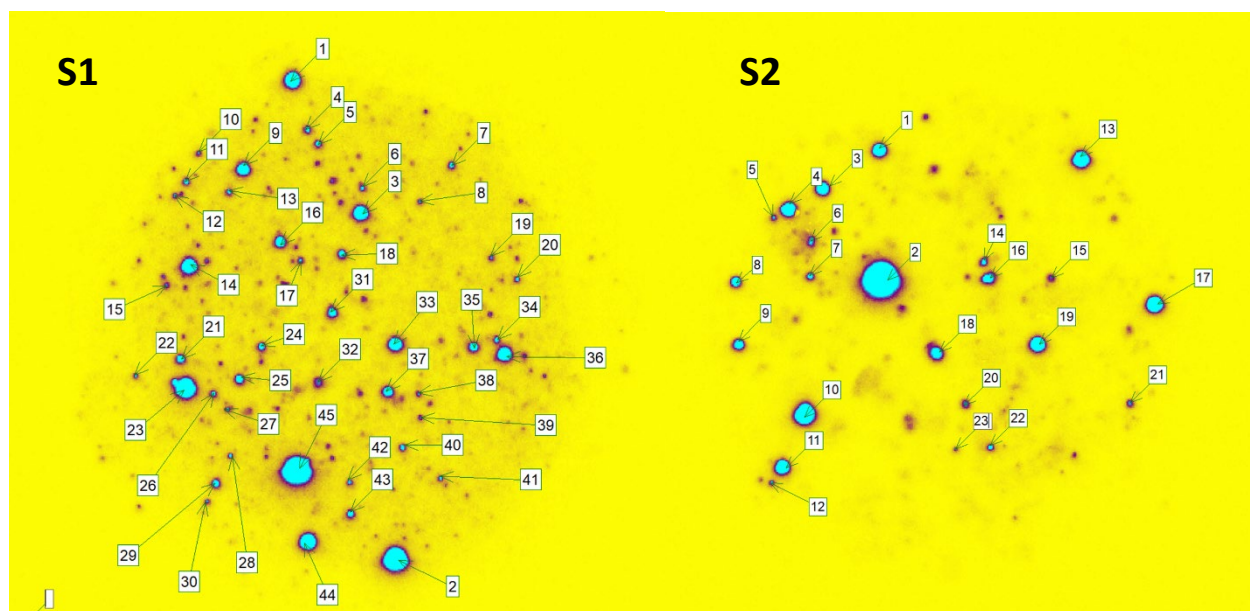
was too low to detect by alpha spectrometry.
However, it is possible that particulate uranium present was high enough to register on the radiograph, and if true would potentially bias particle size determined by this method to a smaller size than actual.

Figure 8: A total of 45 particles in S1 and 23 particles in S2 were identified as accounting for the majority of alpha activity in each sample.

To validate this approach, particle sizes estimated from the radiography data were compared to the particle sizes measured by SEM (Table 2). At the time of this update, only 3 confirmed ^{238}PuO$_2$ particles were found in sample S1 by SEM, and only 2 in sample S2. While the radiography particle sizes are estimated based on a spherical shape, they compare favorably with the dimensions estimated from SEM.

Table 2: Comparison of particle sizes determined by SEM and modeled by radiography

	Estimated Particle Size (µm)	
Particle	SEM (length x width)	Radiography (diameter)
S1-P1	0.98 x 0.56	0.71
S1-P2	2.67 x 1.60	2.1
S1-P3	1.20 x .560	0.73
S2-P1	6.16 x 1.90	1.2
S2-P2	0.96 x 0.73	0.69

The particle size distribution calculated for all 68 particles analyzed shows an average particle size of 0.20 – 0.30 µm, tailing up to 2 µm (Figure 9). The shape of this distribution approximates a log-normal distribution, which is typical of PuO_2 particle samples. The particles found by SEM tend to be at the larger end of this distribution. The discrepancy could be because larger particles are easier to find by SEM, or that the smaller particles in the radiography images are actually uranium particles. This is an area for further investigation, but it is reasonable to assume from the combined SEM and radiography results that most of the $^{238}PuO_2$ particles are < 2 µm.

Particle Size Distribution Estimate for $^{238}PuO_2$
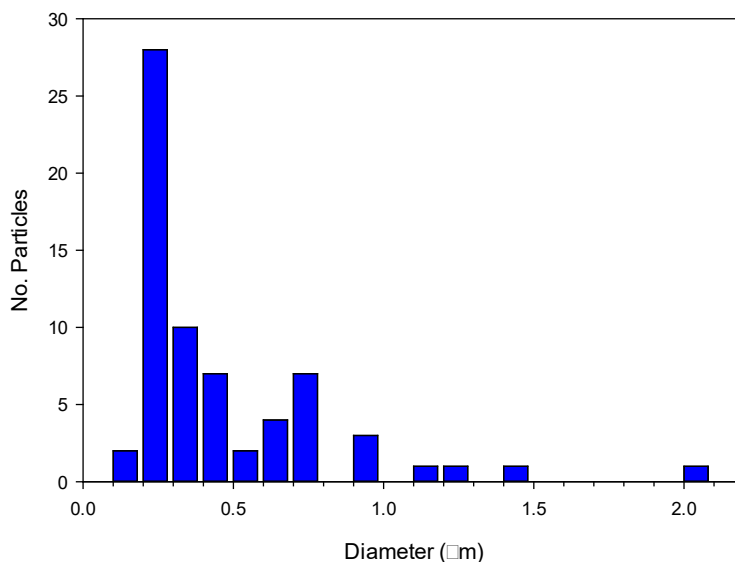68 Particles Removed from PPE

Figure 9: Particle size distribution estimated from radiography data and total ^{238}Pu activity on samples S1 and S2.

6. Solubility study

Sample selection and subdividing

The air sample with the highest ^{238}Pu activity, FAS-32, with approximately 21,000 dpm, was selected for the *in vitro* lung dissolution rate study. This sample was cut into quarters, and each quarter counted by alpha spectrometry to get an initial estimate of the ^{238}Pu activity in each sample (Table 3). While the radiography shows a relatively homogeneous distribution of particles on the filter, the alpha spectrometry of each quarter shows that there is over a factor of 2 variation between the highest quarter and lowest quarter section.

Table3: Total activity of ^{238}Pu measured in the air filter quarters of sample FAS-32

	Total ^{238}Pu	Comb. Unc.	Rel. CU
	[dpm]	[dpm]	[%]
FAS-32 1	7198	148	2%
FAS-32 2	4717	96	2%
FAS-32 3	6221	128	2%
FAS-32 4	3303	69	2%

In vitro lung dissolution rate determination

The experimental approach to determining the *in vitro* lung dissolution rate of Pu in the FAS-32 subsamples generally followed the method used in a previous study of Pu involved in a similar incident at the Savannah River Site [2]. In this case, each of four quarters of the FAS-32 sample were placed into separate containers of simulated lung fluid (SLF) prepared according to the Moss formula (Table 4). The container configuration was chosen to allow full and free contact of the SLF with the samples, and easy separation of SLF fraction collected over the course of the experiment (Figure 10). The samples were placed in an incubator where they were continuously agitated and kept at constant physiological temperature (37 °C) and constant 5% CO_2 atmosphere to stabilize the pH at 7.2 - 7.4.

Table 4: Composition of simulated lung fluid (Moss formula) adjusted to pH 7.2-7.4 with 0.1 mol L^{-1} HCl

Chemical		Concentration [g L^{-1}]
Magnesium chloride	$MgCl_2$ x 6 H_2O	0.203
Sodium chloride	NaCl	6.019
Potassium chloride	KCl	0.298
Sodium phosphate; dibasic*	Na_2HPO_4 x 7 H_2O	0.268
Sodium sulfate	Na_2SO_4	0.071
Calcium chloride**	$CaCl_2$ x 2 H_2O	0.368
Sodium acetate	$NaH_3C_2O_2$ x 3 H_2O	0.952
Sodium bicarbonate	$NaHCO_3$	2.604
Sodium citrate	$Na_3H_5C_6O_7$ x 2 H_2O	0.097

* Anhydrous sodium phosphate was used (0.142 g L^{-1})

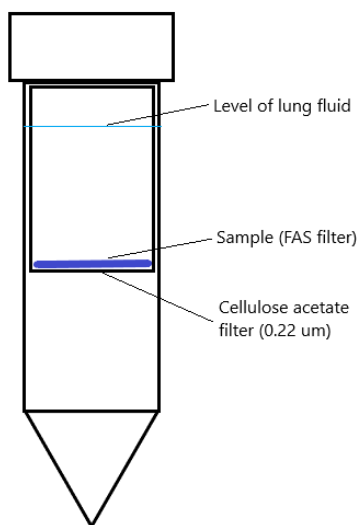** $CaCl_2$ x 4-6 H_2O was used (0.503 g L^{-1})

Figure 10: Centrifuge tube filtration tubes for the solubility study. At each sample change interval, the SLF is removed from the sample by centrifugation, and the filtration insert is transferred to a new tube of SLF.

The study ran for 134 days, with SLF fractions collected and samples transferred to fresh SLF at 0.015, 0.055, 0.23, 1.07, 5.1, 20.1, 43, 77, 100, and 134 days. Fresh SLF was prepared one day prior to, or on the day of sample handling, and the pH of the SLF was adjusted to 7.2 - 7.4 using 0.1 mol L^{-1} HCl just before sample exchange. After collection of the final fraction, the air filter quarters were thermally ashed and dissolved to determine the ^{238}Pu activity remaining undissolved at the end of the study.

Radiochemistry and alpha spectrometry analysis of SLF

The collected SLF fractions were acidified with concentrated HNO_3 and weighed. An aliquot of each subsample was spiked with ~4 dpm ^{242}Pu tracer, evaporated to dryness, and wet ashed with concentrated HNO_3 + 30% H_2O_2 several times to ensure tracer equilibration. The Pu was then radiochemically purified using a two-column procedure that uses ion extraction chromatography followed by ion exchange chromatography. Purified Pu samples were electrodeposited onto stainless steel disks for alpha spectrometry.

With each subsample set, a procedural blank sample was prepared and used to regularly check the pH and re-set it to 7.2 - 7.4 when it was necessary. The procedural blanks were also analyzed together with the subsamples to confirm that no cross-contamination occurred in the incubator, during the radiochemical and alpha spectrometric analysis.

Samples were counted for 2,400 – 10,000 minutes on 300 mm^2 active area Alpha AS detectors. The detectors used for this study had 10,000-minute background counts to confirm that the background at the ^{238}Pu energy range was insignificant. The ^{238}Pu activity was measured relative to the ^{242}Pu tracer added, using the standard LANL bioassay alpha spectrometry data reduction process.

Radiochemistry and alpha spectrometry analysis of FAS air filter quarters and container materials

After the final fractions of the SLF were collected, the FAS air filter quarters were transferred into quartz crucibles, dried, and ashed at 800 °C in a muffle furnace. After an almost one week long extensive acid digestion, the Pu in the samples was fully dissolved. An aliquot of each sample was spiked with [242]Pu tracer, equilibrated, and radiochemically purified by ion exchange chromatography. The purified Pu samples were electrodeposited onto stainless steel disks for alpha spectrometry.

During the air filter transfer, small pieces of the original FAS filters were observed in the bottom and on the wall of the inner container of the centrifuge tubes. Therefore, besides the air filter quarters, the cellulose acetate filters of the centrifuge tubes (Fig. 10) were also decomposed and analyzed in the same way as the air filters (except the maximum ashing temperature was 750 °C).

Finally, the centrifuge tubes that held the FAS filters throughout the whole study, were filled up with approximately 50 mL 8 mol L^{-1} HNO_3 and allowed to sit for 8 days. This removed and dissolved the remaining filter material from the walls of the centrifuge tubes. These solutions were spiked with [242]Pu tracer, equilibrated, radiochemically purified, electrodeposited, and the [238]Pu activities were determined by alpha spectrometry using the same method described above.

Adsorption study to determine potential dissolved [238]Pu loss to surfaces

According to the preliminary results (Report from October 25, 2020 and Memorandum from December 30, 2020), the determined [238]Pu dissolution rate is significantly lower than that of historical data from an earlier study of LANL [238]Pu [2]. As with the earlier test, there was some concern that a fraction of the [238]Pu dissolved during the study could adsorb to surfaces in the centrifuge tubes or re-adsorb onto the filter, which would bias the measured dissolution rate low. Therefore a short adsorption experiment was also performed in parallel to the lung solubility study to determine whether sorption to centrifuge tubes or re-adsorption of already dissolved [238]Pu onto the filter occurred.

The FAS filters have two components: (1) glass fiber and (2) plastic support. For this experiment, these components were separated, cut into four quarters and soaked in 30 mL SLF containing ~2.6 pCi dissolved [238]Pu. There was a procedural blank included in each sample set which did not contain any filter components. The SLF's pH was set to ~7.1 in bulk prior to transferring the SLF into the centrifuge tubes. The sample containers were placed into the incubator where they were continuously agitated and kept at constant physiological temperature (37 °C) and constant 5% CO_2 atmosphere to stabilize the pH. Samples were collected after 5 and 10 days. The SLF and the filter components were separated and analyzed the same way as the FAS-32 samples.

The [238]Pu measured in the procedural blanks and the samples which contained the glass fiber were equal within the overall uncertainties which indicates the dissolved [238]Pu adsorbed onto the wall of the centrifuge tube and not onto the glass fiber. The adsorbed fraction was determined to be ~9.4% of the dissolved [238]Pu after 5 and 10 days, as well and the saturation occurred within 5 days (Figure 11A).
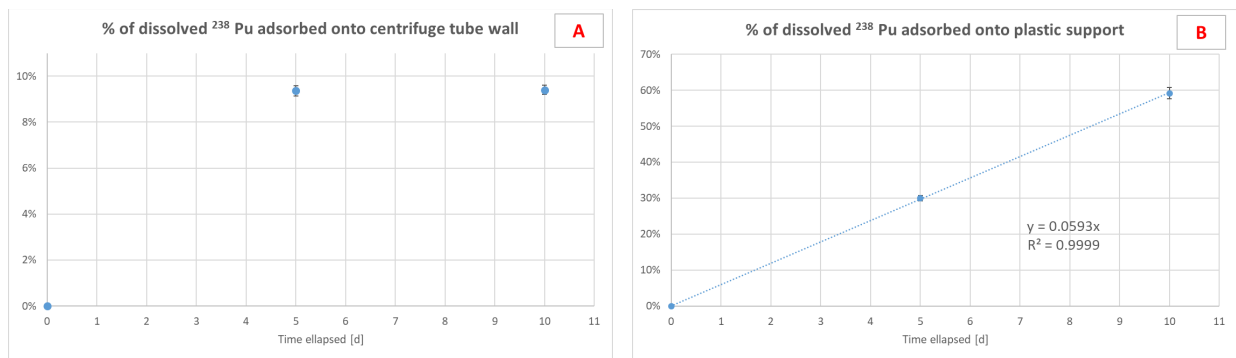
Figure 11: % of dissolved ^{238}Pu adsorbed onto glass fiber (A) and plastic support (B) of the air filter

Approximately ~30% and ~59% of the dissolved ^{238}Pu from the SLF was adsorbed onto the plastic support component of the air filter after 5 and 10 days, respectively. Figure 11B indicates that the adsorption at 10 days was still increasing linearly therefore, it can be concluded that the saturation did not occur within 10 days.

Data analysis

The undissolved ^{238}Pu activity for each filter was calculated by summing the ^{238}Pu activity remaining in the FAS and the small pieces of the FAS stuck to the centrifuge tube filter and walls of the centrifuge tube. This undissolved fraction was added to the sum of the dissolved fractions to provide an initial activity for comparison to the direct alpha spectrometry measurement of the four FAS-32 filter quarters. The fraction of undissolved ^{238}Pu was calculated at each time interval, and used to construct two plots, one showing the fraction of undissolved ^{238}Pu at each time, and a second showing the average fraction ^{238}Pu dissolved/day during each successive sample collection time interval.

The results of the adsorption study were used to estimate the activity of ^{238}Pu that was likely lost to either the walls of the centrifuge tube or re-adsorption to the plastic FAS filter substrate over the course of the study. The worst-case was considered, and employed the following assumptions:

- 0.54 dpm of ^{238}Pu sorbed to the centrifuge tube walls over the first 5 days of the study at which point the active sorption sites were saturated for the duration of the study; and
- The fraction of dissolved ^{238}Pu sorbed per day to the plastic filter substrate followed a linear sorption isotherm with a slope of 0.0593 day^{-1} for the entirety of the study

Using these assumptions, a second set of plots was constructed to show the fraction of undissolved material that included an additional modeled component for the maximum ^{238}Pu likely lost to the centrifuge tube and FAS plastic substrate.

Both sets of curves, along with averages for both of the "as measured" and "isotherm modeled" data sets were fit using the two component exponential function shown in Equation 1.

Equation 1:

$$F = a*e^{-b*t} + c*e^{-d*t}$$

Where: a = fraction of short dissolution half-time material
b = short half-time material rate constant (days^{-1})
c = fraction of long dissolution half-time material
d = long half-time material rate constant (days^{-1})
t = time (days)

This equation was fit to the data in SigmaPlot 14, which uses the Marquardt-Levenberg algorithm to minimize the χ^2 value to find the best fit. Both two and three component exponential functions were tried, and the two component fit was chosen. The three component fit found two fast-dissolving fractions, and the fraction and rate for the long dissolution half-time component in both cases were nearly identical, both indications a three component fit was unnecessary.

Lung dissolution rate results

The total ^{238}Pu activity for each quarter filter is shown in Table 5, which includes the breakdown of undissolved ^{238}Pu, dissolved ^{238}Pu, the total estimated from the destructive analysis of all fractions, and the initial direct measurements by alpha spectrometry for comparison. The initial alpha spectrometry results compared reasonably well with the summed total of the ^{238}Pu activities from the undissolved and dissolved fractions.

Table 5: Activity totals for each sample type used to determine total activity on FAS-32 filter subsamples

		Measured ^{238}Pu activity [dpm]			
		FAS-32 1	FAS-32 2	FAS-32 3	FAS-32 4
Undissolved Fraction Contributors	FAS filters	2498 ± 50 (2.0%)*	2115 ± 42 (2.0%)	5809 ± 107 (1.8%)	2348 ± 48 (2.0%)
	Cellulose acetate filters	267.0 ± 4.3 (1.6%)	684 ± 11 (1.6%)	146.6 ± 2.5 (1.7%)	76.4 ± 1.3 (1.7%)
	Leached samples	640.3 ± 9.2 (1.4%)	794 ± 12 (1.5%)	130.6 ± 2.1 (1.6%)	106.9 ± 1.7 (1.6%)
	FAS-32 D134†	7.72 ± 0.11 (1.4%)	2.919 ± 0.060 (2.0%)	16.32 ± 0.23 (1.4%)	56.69 ± 0.56 (1.0%)
Totals	Total Undissolved ^{238}Pu	7174 ± 73 (1.0%)	4059 ± 45 (1.1%)	6127 ± 107 (1.8%)	3090 ± 49 (1.6%)
	Total Dissolved ^{238}Pu	58.7 ± 1.0 (1.7%)	41.4 ± 1.0 (2.4%)	58.7 ± 1.0 (1.7%)	36.6 ± 1.0 (2.8%)
	Total ^{238}Pu from destructive analysis	7232 ± 73 (1.0%)	4100 ± 45 (1.1%)	6185 ± 110 (1.7%)	3127 ± 49 (1.6%)
	Total ^{238}Pu from direct alpha spec	7200 ± 150 (2.1%)	4717 ± 96 (2.0%)	6210 ± 130 (2.1%)	3303 ± 69 (2.1%)

* Uncertainties are combined standard uncertainties (k=1)
† The D134 fraction showed degradation of the centrifuge filter assembly and breakthrough, therefore was not used in the dissolution rate calculations and added back into the undissolved fraction

The ^{238}Pu activity determined in each fraction collected during the course of the study is shown in Table 6. Originally, the study was planned for 130 days, however, it became apparent from the 134 day fraction results, that there was significant degradation and breakthrough of Pu through the filter used to separate the undissolved Pu particulate from the dissolved Pu in the SLF. Because of this observation, the 134 day fraction activity was added back into the undissolved fraction, and the dissolution rate was only evaluated based on samples collected through 102 days.

Table 6: Analysis results showing the activity of ^{238}Pu dissolved in each fraction during the 102 day *in vitro* study.

Sample ID	Measured ^{238}Pu activity [dpm] in the SLF subsamples			
	FAS-32-1	FAS-32-2	FAS-32-3	FAS-32-4
FAS-32 D0.015	41.58 ± 0.36 (0.9%)*	31.44 ± 0.28 (0.9%)	39.43 ± 0.33 (0.8%)	22.55 ± 0.23 (1.0%)
FAS-32 D0.55	9.26 ± 0.24 (3%)	6.02 ± 0.19 (3%)	9.67 ± 0.24 (2.5%)	4.86 ± 0.14 (3%)
FAS-32 D0.23	4.09 ± 0.17 (4%)	2.00 ± 0.11 (6%)	4.94 ± 0.19 (4%)	6.12 ± 0.22 (4%)
FAS-32 D1.1	1.466 ± 0.093 (6%)	0.571 ± 0.059 (10%)	0.997 ± 0.072 (7%)	0.830 ± 0.070 (8%)
FAS-32 D5.1	0.406 ± 0.026 (6%)	0.091 ± 0.013 (14%)	0.233 ± 0.019 (8%)	0.089 ± 0.013 (15%)
FAS-32 D20.1	1.090 ± 0.036 (3%)	1.229 ± 0.036 (3%)	2.752 ± 0.061 (2.2%)	0.756 ± 0.028 (4%)
FAS-32 D43	0.226 ± 0.014 (6%)	0.0843 ± 0.0087 (10%)	0.328 ± 0.016 (5%)	0.264 ± 0.014 (5%)
FAS-32 D77	0.318 ± 0.017 (5%)	0.0254 ± 0.0047 (18%)	0.196 ± 0.012 (6%)	0.634 ± 0.024 (4%)
FAS-32 D102	0.252 ± 0.015 (6%)	0.0528 ± 0.0088 (17%)	0.157 ± 0.012 (8%)	0.527 ± 0.020 (4%)
FAS-32 D134†	7.72 ± 0.11 (1.4%)	16.32 ± 0.23 (1.4%)	2.919 ± 0.060 (2.0%)	56.69 ± 0.56 (1.0%)

* Uncertainties are combined standard uncertainties (k=1)
† The D134 fraction showed degradation of the centrifuge filter assembly and breakthrough, therefore was not used in the dissolution rate calculations and added back into the undissolved fraction

There also appears to be a higher than expected activity in the day 20 fractions, likely caused by the adsorption of ^{238}Pu to the centrifuge walls up through day 5, and before the sorption of ^{238}Pu onto the FAS plastic substrate had any significant impact. This scenario is supported by Figures 12A-C, where a higher daily dissolution rate is present at 20 days in the "as measured" data. When a simple linear isotherm model is applied to account for ^{238}Pu adsorption to the FAS plastic substrate, the daily dissolution rate for the later fractions is higher, but has little impact on the earlier fractions. However, when both the linear isotherm FAS plastic substrate and the centrifuge tube sorption component are included, the first 5 days show behavior closer to expected, where the daily dissolution rate is gradually decreasing through the study.

Rate of ^{238}Pu dissolution/day for each sample collection interval
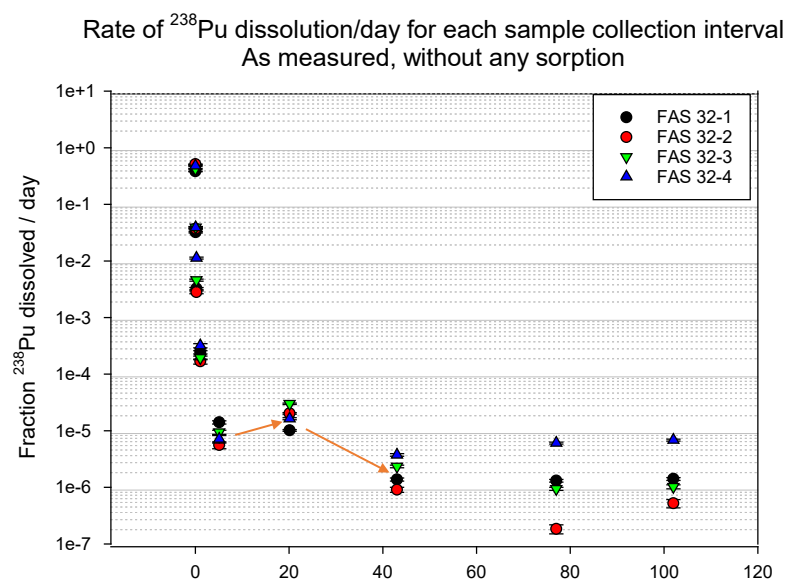### As measured, without any sorption

Figure 12A: Daily dissolution rate for each collection interval as measured. Note the apparent rise in daily dissolution rate between days 5 and 20, before it falls off and stabilizes at day 40 (orange arrows).
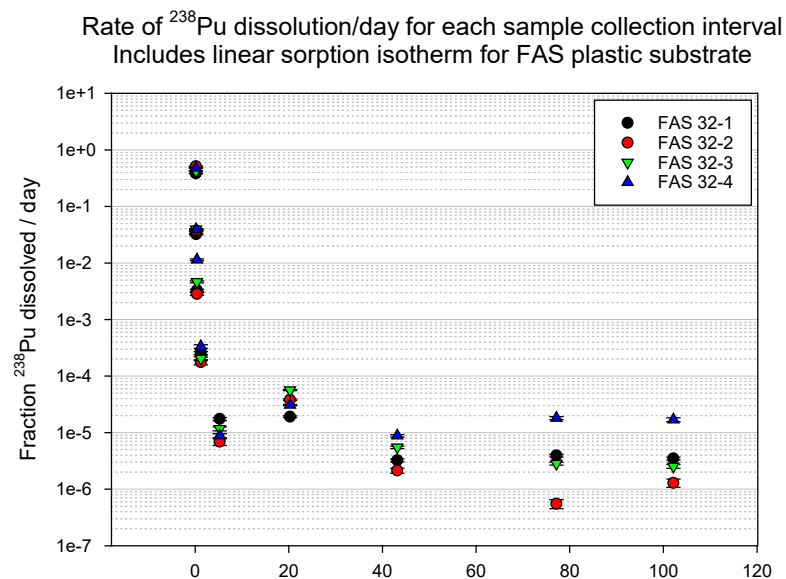
Rate of ^{238}Pu dissolution/day for each sample collection interval
Includes linear sorption isotherm for FAS plastic substrate

Figure 12B: Daily dissolution rate for each collection interval that includes both measured ^{238}Pu activity, and a modeled component to account for ^{238}Pu re-adsorbed to the FAS plastic substrate. This has minimal impact on the apparent rise in dissolution rate between days 5 and 20, but does elevate the estimated daily dissolution rates beyond day 40.

Rate of ^{238}Pu dissolution/day for each sample collection interval
Includes both centrifuge tube and FAS plastic substrate sorption
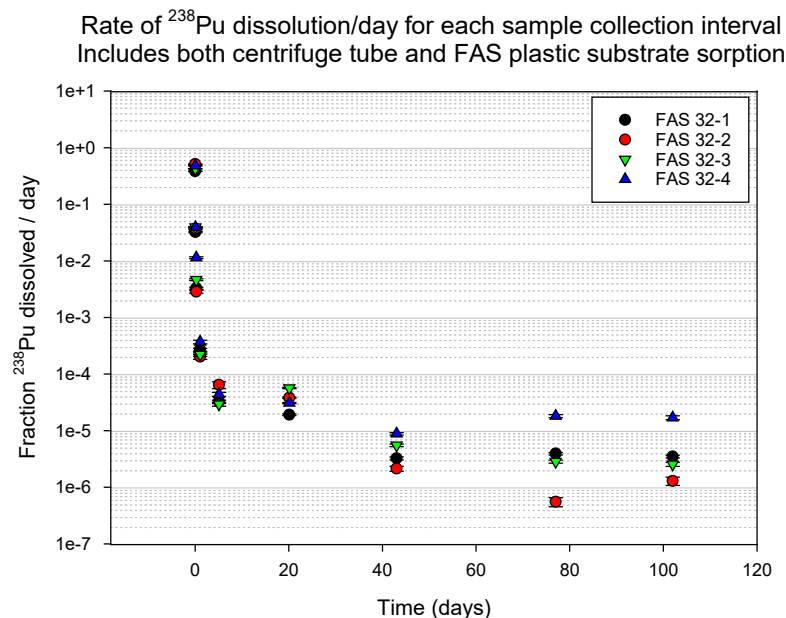
Figure 12C: Daily dissolution rate for each collection interval that includes both measured ^{238}Pu activity, and modeled components to account for both ^{238}Pu re-adsorbed to the FAS plastic substrate, and faster sorption of ^{238}Pu to the centrifuge tube walls. This elevates the daily dissolution rate through day 5 sufficiently to produce the gradual decline in daily dissolution rate expected for a highly insoluble material.

A comparison of the dissolution curves for the directly measured data and the data adjusted for sorption is shown in Figure 13. While there is a clear difference between the measured and modeled data, the differences are relatively small compared to the overall uncertainty in estimating a dissolution rate for a highly-insoluble material from a 100 day study. The slightly different behavior between subsamples is also commonly observed in *in vitro* studies [1,2], and is probably the result of slightly different particle size distributions on each FAS subsample. This is potentially a more substantial issue for a high-specific activity material like $^{238}PuO_2$, where the number of particles on each subsample is relatively small, and not necessarily statistically consistent with overall particle population characteristics. The same dissolution rate data is shown in Figure 14, with several fit results included. Table 7 details the results of the four fit lines shown on the plot in Figure 14.
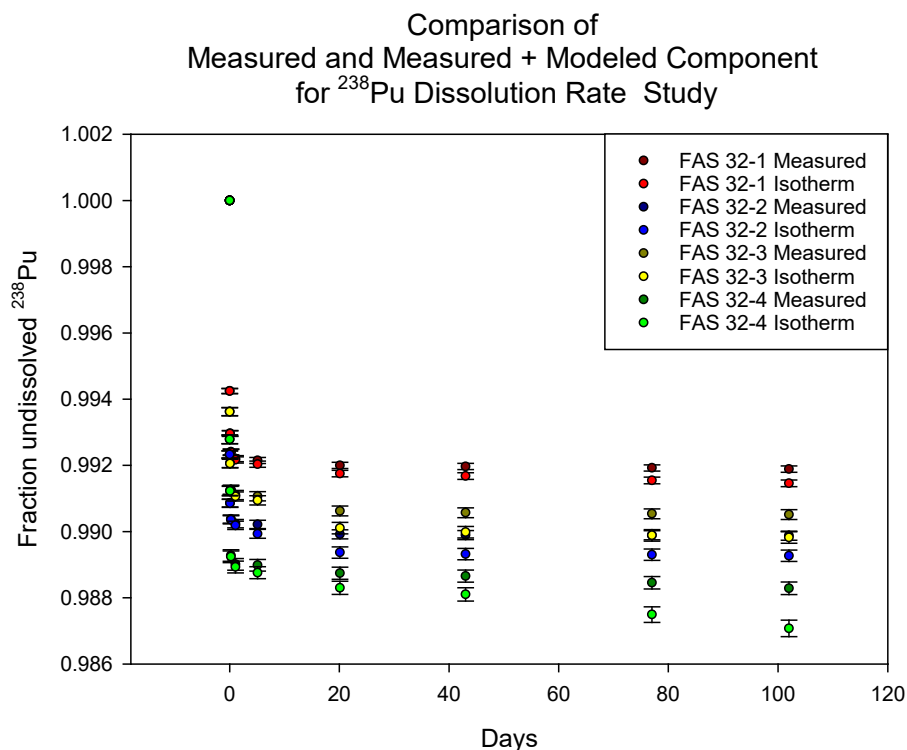

Figure 13: Fraction of ^{238}Pu in the undissolved fraction over the course of the study. This data set includes both the "as measured" and "isotherm modeled" data sets for each of the four subsamples of FAS 32.

Table 7: Summary of fit results detailing the dissolution behavior for the $^{238}PuO_2$ studied

	Rapid fraction	Rapid rate (d^{-1})	Slow Fraction	Slow rate (d^{-1})
Slowest dissolution boundary rates	0.0076 ± 0.0001	90.9 ± 9.5	0.9924 ± 0.0001	5.7E-06 ± 2.5E-6
Mean rates (as measured)	0.0092 ± 0.0002	86 ± 11	0.9908 ± 0.0002	8.5E-06 ± 3.7E-6
Mean rates (w/ isotherm model)	0.0093 ± 0.0002	84 ± 12	0.9907 ± 0.0002	1.54E-05 ± 4.4 E-6
Fastest dissolution boundary rates	0.0107 ± 0.0003	68 ± 13	0.9893 ± 0.0003	2.41E-05 ± 7.0E-6

Comparison of
Measured and Measured + Modeled Component
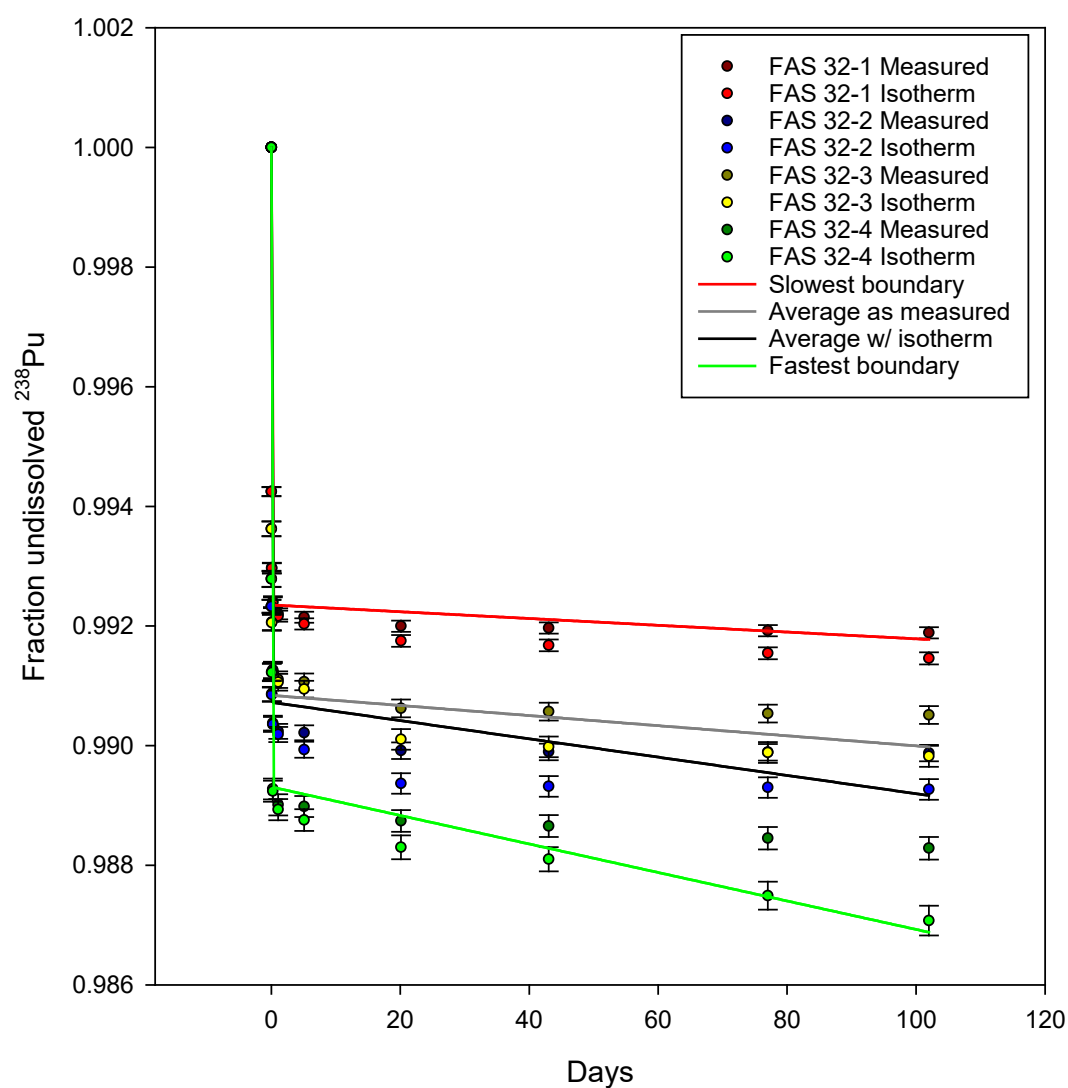for $^{238}PuO_2$ Dissolution Rate Study

Figure 14: Dissolution curves and fit results for select cases from the study. The samples with the lowest and highest slow dissolution rates were fit as boundary conditions (red and green), along with a fit of the average "as measured" data (grey), and a fit of the average "isotherm modeled" data (black).

Summary

The results of this *in vitro* experiment show the $^{238}PuO_2$ released during the incident has a small component of rapidly dissolving material, while approximately 99% of the material dissolves at a slow rate of 1.5×10^{-5} day^{-1}. This is both significantly slower than the one previous measurement of LANL $^{238}PuO_2$ (6.09×10^{-4} day^{-1}) [1], and the ICRP 66 defined Type S material (1.0×10^{-4} day^{-1}) [3], however it is also significantly faster than rates measured for $^{239}PuO_2$ (5.8×10^{-7} day^{-1}) [2]. These differences are not unexpected, and are a combined function of a number of material specific characteristics, including specific activity, material age, particle size distribution, specific surface area, and calcine temperature.

In the case of the $^{238}PuO_2$ for this study, its lower dissolution is likely attributable to it having been freshly prepared and calcined. Given the nature of the release, it is impossible to attribute the released material to a single source of material. However, it is likely the material was associated with the furnace used to calcine $^{238}PuO_2$, and from either the most recent batch processed or a combination of batches from material hold-up in the furnace. The small rapidly dissolving fraction indicates the material likely had a higher degree of crystallinity than an aged material, where crystallinity would have been gradually compromised from damage caused by recoil during alpha decay of the ^{238}Pu [4]. The much higher specific activity of ^{238}Pu than ^{239}Pu (or weapons grade Pu) is considered the reason $^{238}PuO_2$ shows faster dissolution rates than $^{239}PuO_2$, which would also support the argument that older material would have a faster dissolution rate than fresh material. Unfortunately, the calcination temperature and date was not published for the previous study of LANL material [1], so it is not possible to draw a more definitive conclusion on this hypothesis. Overall, this study highlights the need to develop a better understanding how the material characteristics of $^{238}PuO_2$ influence lung dissolution rates, and how those characteristics change with calcine temperature, particle size distribution, and material age.

References

1. Cheng, Y.S.; Guilmette, R.A.; Zhou, Y.; Gao, J.; LaBone, T.R.; Whicker, J.J.; and Hoover, M.D. "Characterization of Plutonium Aerosol Collected During an Accident." *Health Phys.* 87 (2004) 596-605.
2. LaMont, S.P.; LaBone, T.R.; Cadieux, J.R.; Findley, W.M.; Hall, G.; Shick, C.R.; Efurd, D.W.; and Steiner, R.E. "In Vitro lung dissolution rates for PuO$_2$." *J. Radioanal. Nucl. Chem.* 269, 2 (2006) 271-277.
3. International Commission on Radiological Protection. "Human respiratory tract model for radiological protection." Oxford: Elsevier Science Ltd.' Ann. ICRP 24 (1-4) Publication 66 (1994).
4. LaMont, S.P.; Filby, R.H.; Glover, S.E. "*In Vitro* Dissolution Characteristics of Aged and Recrystallised High-Fired $^{232}ThO_2$." *Radiat. Prot. Dosim.* 97, 2 (2001) 161-168.

Appendix 1:

Radiochemical procedure for the determination of Pu in SLF

At the beginning of the study, 20 mL SLF was added into the lower part of the centrifuge tubes, then the inner container was inserted. The quarters of the air filter were placed into the inner container. After 10 mL SLF was added, the centrifuge tubes were centrifuged 3 times at <1500 rpm for 2 minutes. Finally, the inner container was filled with an additional 19.5 mL SLF. The cap of the centrifuge tubes were punctured before the samples were placed into the incubator to let the sample medium interact with the CO_2 atmosphere. The samples were continuously agitated and kept at constant physiological temperature (37 °C) and constant 5% CO_2 atmosphere to stabilize the pH at 7.2 - 7.4.

At every sample collection, the same procedure was followed using freshly prepared (on the day or the day before the sample collection) and pH adjusted SLF using 0.1 mol L^{-1} HCl. The subsamples were collected and the FAS filter quarters were soaked in fresh SLF at the following time intervals:

- Day 0.015 (Sample ID: D0.01),
- Day 0.055 (Sample ID: D0.1),
- Day 0.23 (Sample ID: D0.25),
- Day 1.07 (Sample ID: D1),
- Day 5.1 (Sample ID: D5),
- Day 20.1 (Sample ID: D20),
- Day 43 (Sample ID: D43),
- Day 77 (Sample ID: D77),
- Day 100 (Sample ID: D100),
- Day 134 (Sample ID: D134).

The collected SLF portions were always acidified with 5.5 mL concentrated HNO_3 and transferred into a weighed HDPE bottle. Approximately 33% - 60% of the subsamples were analyzed and the rest archived.

After spiking with ~4 dpm ^{242}Pu, the SLF subsamples were evaporated to dryness and wet ashed with concentrated HNO_3 and 30% H_2O_2 several times. The residue was dissolved in 25 mL 2.5 mol L^{-1} HNO_3 / 0.075 mol L^{-1} sulfamic acid / 0.15 mol L^{-1} ascorbic acid. After complete dissolution, ~300 µg Fe(III) was added in the form of $Fe(NO_3)_3$ x 9 H_2O dissolved in 1 mol L^{-1} HNO_3 (5 mg Fe(III)/mL). In this media, Pu was reduced to Pu(III) within a short period of time. After 5 minutes, approximately 100-150 mg $NaNO_2$ was added to the samples which turned trivalent Pu into the tetravalent state. Samples were loaded after approximately 30-45 minutes onto a 2-mL TRU Spec® (100-150 µm) column rinsed with 10 mL 0.025 mol L^{-1} HNO_3 and conditioned with 10 mL 2.5 mol L^{-1} HNO_3. During the waiting time, the samples needed to be mixed thoroughly to remove all bubbles formed by $NaNO_2$. After loading, the sample vials were rinsed with 5 mL 2.5 mol L^{-1} HNO_3 and added onto the TRU Spec® column. The column was then rinsed with 10 mL 2.5 mol L^{-1} HNO_3 / 0.5 mol L^{-1} $H_2C_2O_4$ (oxalic acid). Plutonium was eluted with 15 mL 0.025 mol L^{-1} HNO_3 and 15 mL 0.1 mol L^{-1} $NH_4HC_2O_4$ (ammonium bioxalate).

The Pu fractions were evaporated to dryness overnight and ashed at 450 °C for one hour in a muffle furnace. After several steps of wet ashing with concentrated HNO_3 and 30% H_2O_2, the residue was dissolved in 10 mL 8 mol L^{-1} HNO_3. The samples were heated at approximately 100 °C for 10 minutes and allowed to cool for an additional 50 minutes. The samples were then loaded onto a 2-mL AG 1-x4 (100-

200 mesh) column which was previously rinsed with 10 mL 9 mol L^{-1} HCl, 10 mL 0.1 mol L^{-1} HCl, 10 mL 18.2 MΩ water and conditioned with 30 mL 8 mol L^{-1} HNO$_3$. After loading, the column was further rinsed with 25 mL 8 mol L^{-1} HNO$_3$ (the first 5 mL was used to rinse the sample vials) and 20 mL 9 mol L^{-1} HCl. Finally, Pu was eluted with either 20 mL concentrated HBr (subsamples day 0.015 … day 20.1) or 20 mL 9 mol L^{-1} HCl / 0.1 mol L^{-1} NH$_4$I (subsamples day 44 … 100).

The samples were evaporated to dryness and wet ashed with aqua regia (only in case the Pu elution was done in the presence of NH$_4$I), concentrated HNO$_3$ and 30% H$_2$O$_2$ several times. Then 2 mL 5% NaHSO$_4$ and 1 mL concentrated HNO$_3$ were added and evaporated to dryness and finally, dissolved in 4 mL 15% Na$_2$SO$_4$. The samples were then loaded into the electrodeposition cells and diluted with 18.2 MΩ water to approximately 10-12 mL. The alpha source preparation procedure was performed at 0.5 A current for 3 hours. The samples were then counted typically for 2,400 – 10,000 minutes using 300 mm^2 active area Alpha AS detectors.

Appendix 2:

Radiochemical procedure for the determination of Pu in FAS filters

After the final fractions of the SLF were collected, the air filter quarters were transferred into a quartz crucible. The inner containers of the centrifuge tubes had to be disassembled to recover the cellulose acetate filters. These filters were also placed into quartz crucibles. Each piece of the inner container was placed into a new centrifuge tube and filled up with approximately 50-55 mL 8 mol L^{-1} HNO_3. The nitric acid was left for 8 days in the centrifuge tubes to dissolve any remaining material in the tubes. Afterwards the entire volume was evaporated to dryness in quartz crucibles.

The filters were dried overnight in the crucibles with the cap on due to the high ^{238}Pu activity. They were then ashed in a muffle furnace with the following protocol:

- At 105 °C for ~1 hour,
- At 300 °C for ~1 hour,
- At 400 °C for ~4 hours,
- At 600 °C for ~4 hours (cellulose acetate filters) / for ~6 hours (FAS filters),
- At 700 °C for ~3 hours (cellulose acetate filters) / for ~6 hours (FAS filters),
- At 750 °C for ~5 hours (cellulose acetate filters) / at 800 °C for ~7 hours (FAS filter quarters).

The high temperature ashing took several days (4 - 7 days) and at the end of each day the muffle furnace was turned off.

After ashing the filters and evaporating the leaching solutions, 4 - 8 mL 8 mol L^{-1} HNO_3 was added into the quartz crucibles. The samples were heated at 95-120 °C for a few hours. The evaporated portion of the nitric acid was refilled, and at the end, 200 µL concentrated HF was added. The samples were heated until all ashed residue was removed from the wall of the quartz crucibles. Due to the presence of HF, the quartz crucible was etched, as well. The samples were then transferred into a 22-mL Teflon vial and the quartz crucibles were rinsed twice with a small volume of 8 mol L^{-1} HNO_3.

After the samples were evaporated to dryness, they were wet ashed with different acid mixtures:

- 2 mL 1:1 mixture of concentrated HNO_3 and concentrated HF,
- 1.5 mL aqua regia (1:3 mixture of concentrated HNO_3 and concentrated HCl),
- 2 x 2 mL of concentrated HNO_3 and 120 uL 30% H_2O_2,
- 2 mL of concentrated HNO_3.

After the evaporation of the concentrated HNO_3, the sample residues were dissolved in 4 mL, 10 mL and 1 mL 8 mol L^{-1} HNO_3 in case of the cellulose acetate filters, FAS filters and the leached samples, respectively. Approximately 50% of the cellulose acetate filters, 5% of the FAS filters and 100% of the leached samples were then used for further analysis. For the cellulose acetate filters and leached samples, approximately 4 dpm ^{242}Pu was used as tracer; for the FAS filters approximately 45 dpm. After sample splitting and spiking, the samples were slowly dried up to reach equilibrium between the Pu in the samples and the tracer solution.

The residue of the samples was dissolved in 10 mL 8 mol L^{-1} HNO$_3$. The samples were heated at approximately 100 °C for 10 minutes and allowed to cool for an additional 50 minutes. The samples were then loaded onto 2-mL AG 1-x4 (100-200 mesh) columns previously rinsed with 10 mL 9 mol L^{-1} HCl, 10 mL 0.1 mol L^{-1} HCl, 10 mL 18.2 MΩ water and conditioned with 30 mL 8 mol L^{-1} HNO$_3$. After loading, the column was further rinsed with 25 mL 8 mol L^{-1} HNO$_3$ (the first 5 mL was used to rinse the sample vials) and 20 mL 9 mol L^{-1} HCl. Finally, Pu was eluted with 20 mL 9 mol L^{-1} HCl / 0.1 mol L^{-1} NH$_4$I.

The samples were evaporated to dryness and wet ashed with small volumes of aqua regia, concentrated HNO$_3$ and 30% H$_2$O$_2$ several times. Then 2 mL 5% NaHSO$_4$ and 1 mL concentrated HNO$_3$ were added and evaporated to dryness and finally, dissolved in 4 mL 15% Na$_2$SO$_4$. The samples were then loaded into the electrodeposition cells and diluted with 18.2 MΩ water to approximately 10-12 mL. The alpha source preparation procedure was performed at 0.5 A current for 3 hours. The samples were then counted typically for 240 – 2,800 minutes using 300 mm^2 active area Alpha AS detectors.

After the analysis, residue was still observed from the filters in the original quartz crucibles which were used during the ashing. It became visible only after they were completely dry. Therefore all quartz crucibles which were used for ashing of both filter types were leached with 8 mol L^{-1} HNO$_3$. All samples were kept warm during working hours at 80-100 °C for two days. The evaporated nitric acid was always refilled. Finally, 400 µL concentrated HF was added to each sample and kept them in the quartz crucibles until the entire ashed residue of the filters was removed from the wall of the quartz crucibles. The quartz crucibles were double-checked to see if there was any remaining residue from the ashed filters.

The leaching of the inner container was also repeated.

After the wet digestion with the different acid mixtures was completed the samples were combined and the same procedure was applied as discussed above. In Appendix 3, they are referred to as 'Combined samples'.

Appendix 3:

Radiochemical analysis quality control information

Two types of procedural blanks (PB) were analyzed with every batch of samples.

Type I procedural blanks were matrix matched blank samples which were treated as real samples. They also spent the same time period in the incubator as the samples themselves. They were also used to regularly check and adjust the pH of the SLFs in the incubator. Their other purpose was to detect whether cross-contamination happened during the study and sample preparation.

Type II procedural blanks contained only ~4 dpm ^{242}Pu and only went through the electrodeposition procedure to prepare alpha sources. Their main purpose was to determine the Pu recovery of the electrodeposition step. They were, however, placed onto the hot plate as soon as the radiochemical procedure of the certain batch of samples was started. So they were exposed to the laboratory environment during the whole sample preparation.

The average ^{238}Pu activity measured in the procedural blanks - analyzed together with the SLF subsamples - were identical within the uncertainties:

- PB Type I: 0.00169 ± 0.00048 dpm (28%) (k=1; n = 8),
- PB Type II: 0.00114 ± 0.00069 dpm (60%) (k=1; n = 8).

Figure 1 and Table 1 (values marked with red) show evidence for cross-contamination but only in case of the PB Type I of the SLF subsamples FAS-32 1 … 4 D100 counts as significant when the level is compared to the ^{238}Pu activity range in analyzed sample aliquots.
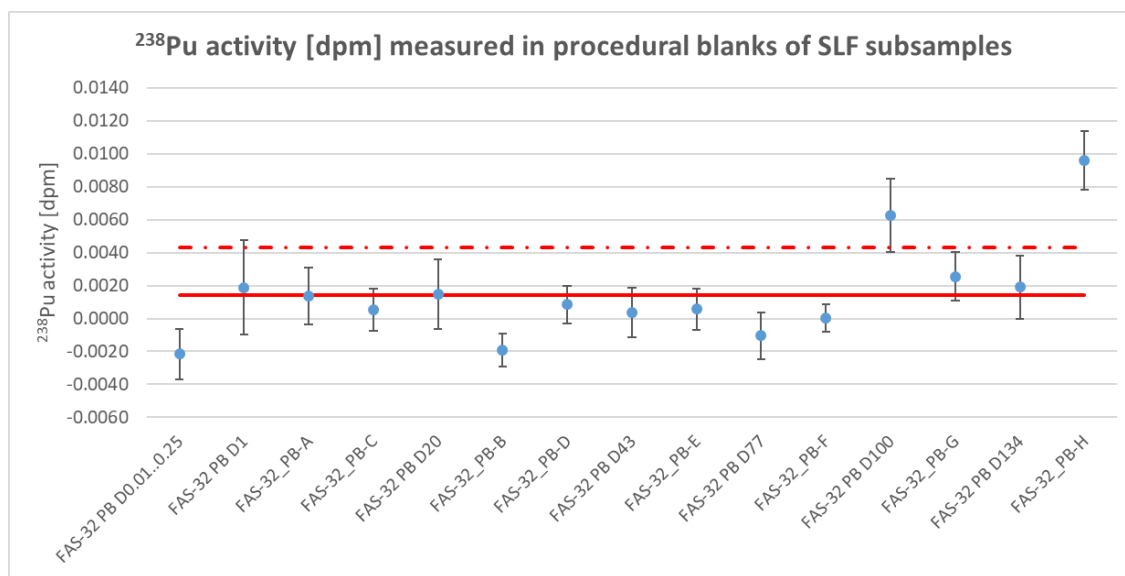

Figure 1: ^{238}Pu activity measured in the procedural blanks of the SLF subsamples
Red line represents the average of the PB level and
the dashed red line represents the level of average + one standard deviation.

Table 1: ^{238}Pu activity measured in the procedural blanks and compared to the ^{238}Pu activity range measured in the analyzed sample aliquots of the filter samples

	^{238}Pu activity in PB Type I [dpm]	^{238}Pu activity PB Type II [dpm]	^{238}Pu activity range in analyzed aliquots [dpm]
FAS-32 1 … 4 D100	0.0063 ± 0.0022 (35%)*	0.0026 ± 0.0015 (58%)	0.053 - 0.527
FAS-32 1 … 4 D134	0.0019 ± 0.0019 (100%)	0.0096 ± 0.0018 (19%)	2.9 - 56.7

* Combined standard uncertainty (k = 1)

The ^{238}Pu activity measured in the procedural blanks of the filter samples are significantly higher than that of the SLF subsamples (Table 2). Their activity level (-0.0019 - 0.776 dpm), however, negligible compared to the ^{238}Pu activity range in analyzed sample aliquots (38 - 640 dpm).

Table 2: ^{238}Pu activity measured in the procedural blanks and compared to the ^{238}Pu activity range measured in the analyzed sample aliquots of the filter samples

	^{238}Pu activity in PB Type I [dpm]	^{238}Pu activity PB Type II [dpm]	^{238}Pu activity range in analyzed aliquots [dpm]
FAS filters	0.0225 ± 0.0060 (27%)*	0.0244 ± 0.0052 (21%)	110 - 30
Cellulose acetate filters	0.776 ± 0.044 (6%)	-0.0019 ± -0.0014 (72%)	38 - 347
Leached samples	0.171 ± 0.014 (8%)	0.0090 ± 0.0039 (43%)	107 - 640

* Combined standard uncertainty (k = 1)

Pu recoveries

All radiochemical procedures used in the lung solubility study were tested and optimized to the specific samples matrices prior to their use on the FAS-32 samples. The method development was performed parallel to the lung solubility study.

The SLF samples of batches from FAS-32 D0.01 to FAS-32 D20 were prepared using the radioanalytical procedure including the two-step Pu separation using concentrated HBr as the Pu eluant in the second separation step. We observed that the achieved total Pu recoveries were low and they varied in a wide range, between 30% and 62%.

After performing a few test analyses, HBr was identified to be responsible for the low Pu recoveries. In order to improve the recoveries, several Pu eluants were tested and using 9 mol L^{-1} HCl / 0.1 mol L^{-1} NH$_4$I showed the highest Pu recoveries (>90%), therefore HBr was replaced with this new Pu eluant in the rest of the solubility study whenever the Pu separation was done on a BioRad AG 1x4 column. The Pu recoveries showed improvement (Table 3), even though the analyzed sample aliquots increased from ~33% to ~60% from batch FAS-32 D43.

The Pu recoveries of the electrodeposition step varied between 88% and 93%.

Table 3: Pu recoveries of the SLF subsamples

Sample ID	Total Pu recovery [%]					
	FAS-1	FAS-2	FAS-3	FAS-4	PB type I	PB type II
FAS-32 D0.01	50%	51%	51%	44%	58%	89%
FAS-32 D0.1	49%	48%	54%	62%		
FAS-32 D0.25	34%	34%	36%	35%		
FAS-32 D1	35%	35%	40%	34%		
FAS-32 D5	33%	33%	34%	30%	45% / 48%	92% / 90%
FAS-32 D20	48%	54%	51%	54%	50%	89%
FAS-32 D43	56%	64%	58%	65%	67%	88%
FAS-32 D77	52%	66%	60%	52%	70%	88%
FAS-32 D100	52%	45%	45%	58%	62%	88%
FAS-32 D134	58%	48%	42%	69%	64%	93%

The recoveries of the filter samples were significantly higher since there was only a one-step Pu separation performed. The achieved total Pu recoveries varied between 75% and 90%, while the Pu recoveries of the electrodeposition step varied between 89% and 93%.